

# MODELLING A HORMONE-BASED ROBOT CONTROLLER

Thomas Schmickl, K. Crailsheim

Department of Zoology, Karl-Franzens University Graz, 8010 Graz, Universitätsplatz 2, Austria

Corresponding author: Thomas Schmickl, Artificial Life Lab of the Department of Zoology, Karl-Franzens University Graz, 8010 Graz, Universitätsplatz 2, Austria, [thomas.schmickl@uni-graz.at](mailto:thomas.schmickl@uni-graz.at)

**Abstract.** For all living organisms, the ability to regulate internal homeostasis is a crucial feature. This ability to control variables around a set point is found frequently in the physiological networks of single cells and of higher organisms. Also nutrient allocation and task selection in social insect colonies can be interpreted as homeostatic processes of a super-organism. And finally, also behaviour can represent such a control scheme. We show, how a simple model of hormone-regulation, inspired by simple biological organisms, can be used as a novel method to control the behaviour of autonomous robots. We demonstrate the formulation of such an 'artificial homeostatic hormone system' (AHHS) by a set of linked difference equations and we explain how the homeostatic control of behaviour is achieved by homeostatic control of the internal 'hormonal' state of the robot. The test task that we used to check the quality of our AHHS controllers was a very simple one, which is often a core functionality in controller programs that are used in autonomous robots: obstacle avoidance. We demonstrate two implementations of such an AHHS controller that perform this task in differing levels of quality. Both controllers use the concept of homeostatic control of internal variables (hormones) and they extend this concept to include also the outside world of the robots into the controlling feedback loops: As they try to regulate internal hormone levels, they are forced to keep a homeostatic control of sensor values in a way that the desired goal 'obstacle avoidance' is achieved. Thus the created behaviour is also a manifestation of the acts of homeostatic control. The controllers were evaluated by using a stock-and-flow model, that allowed sensitivity analysis and stability tests. In addition to that, we have tested both controllers also in a multi-agent simulation tool, which allowed us to predict the robots' behaviours in various habitats and group sizes. The examples shown in this article represent a first step in our research towards autonomous aggregation and coordination of robots to higher-level, modular robotic organisms, that consist of several joined autonomous robotic units. In the end we plan to achieve such aggregation patterns also by using AHHS controllers, as they are described here.

## 1 Introduction

For the swarm robotic project I-SWARM [12], we developed algorithms that allowed a swarm of autonomous robots to aggregate at a target without a central unit of control. In our current projects SYMBRION [15] and REPLICATOR [9] we have the aim to create a swarm of small autonomous robots able to generate autonomously moving higher-level robotic organisms by joining together many individual robots to one structure. The process how these robotic modules navigate throughout the environment and how they interact (communicate) with each other will not be pre-programmed. In contrast, at the end it will be a self-organized process shaped by artificial evolution.

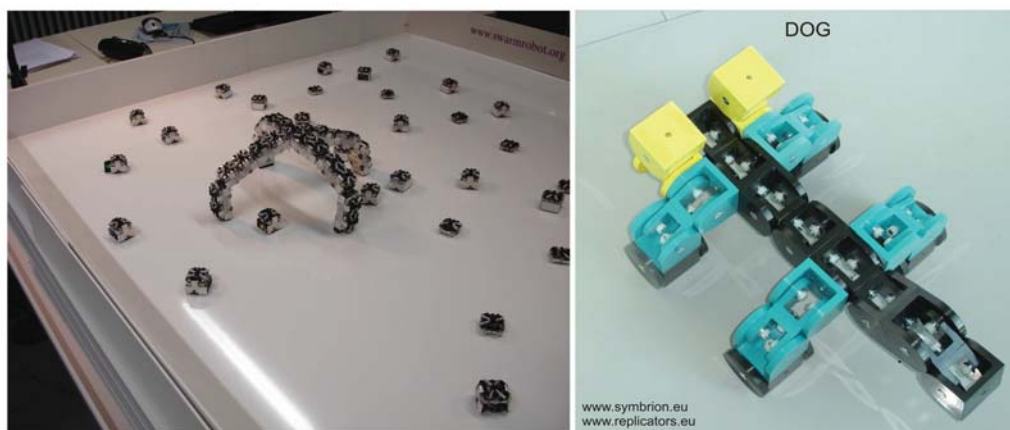


**Figure 1:** Left: A swarm of autonomous JASMINE robots [10], partially aggregated to a multi-modular robot organism. The AHHS controller presented here first aim is to control the swarm of individually driving robot units. Right: Example configurations of several joined robotic units to a higher level organism, constructed from dummy modules. In the later development, we plan to use a network of joint AHHS controllers to regulate internal homeostasis and motion of such aggregated robotic organisms. Photos courtesy of Dr. Kernbach, University of Stuttgart.

We describe here how a novel bio-inspired robot controller allows the robot to develop reaction patterns which result from the received sensory input. The controller is inspired by physiological processes found in living organisms (hormones) or within single cells (second messengers). In recent years hormone-inspired approaches have been suggested for robot controllers for multiple purposes: Navigation of single robots [6], coordination of multi-modular robots [14] or, sometimes also called pheromone-based [7] or trophallaxis-based controllers, for the coordination of robot swarms [11].

We claim that hormone-controllers mimicking the dynamics of fluid concentrations have three main advantages: First, they allow internal homeostasis resulting from interwoven positive and negative feedback loops. Second, when equilibrium is disturbed by a sudden event, they automatically converge to a new homeostatic set point. Third, evolutionary algorithms can operate on a smooth fitness landscape that is advantageous for numerical optimization. Our suggested novel algorithm simulates such floating hormones and uses an internal compartmentalization of the robot by incorporating also a diffusion process of our 'hormones'. Our studies on real robotic hardware and with robot simulators showed that such a bio-inspired 'artificial homeostatic hormone system' (AHHS) is well suited to navigate robots and to coordinate (and aggregate) robot swarms to specific (body-) shapes. In this article we demonstrate the basic abilities of such an AHHS with a simple mathematical representation, which can be either a set of linked ordinary differential equations or a set of difference equations which fit well to the stepwise execution of robot programs.

## 2 The Robot Controller

The basic idea of our AHHS-based robot controller is that sensory input to the robot triggers the excretion of specific hormones, which are internally represented by numeric variables. The virtual internal space of the robot can consist of several compartments, thus an array (or matrix) is internally used to hold the hormone levels for all compartments.

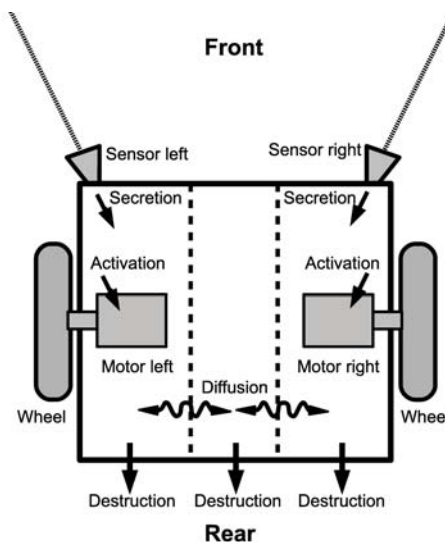


**Figure 2:** Schematic representation of the way our hormone controller assumes an internal compartmentalization of the robot's body. Sensors excrete hormones into one compartment, actuators get activated by local hormone concentrations and hormones diffuse between compartments.

Each hormone has a base production rate and a fixed decay rate. These two processes of production and decay lead already to a hormone-specific equilibrium that is approached by the system. These homeostatic set points can be shifted by additional hormone input which is triggered by sensor inputs. Sensors only affect the hormone secretion in the compartment they are associated with, but all hormones spread through the system by diffusing to neighbouring compartments with a fixed hormone-specific diffusion coefficient. See figure 2 for a schematic picture that describes, how the robot is assumed to be (virtually) compartmentalized, and how sensors and actuators are linked to specific compartments. In figure 2 we show how a simple robot, which is driven by two wheels (differential drive) and which has 2 distance-sensors pointing in a lateral-frontal direction, can be represented by an AHHS controller: We assume that the internal space of the robot is best reflected by 3 compartments. The left one holds the left sensor and the left motor and the right compartment holds the right sensor and the right motor. A central compartment acts as a time delaying compartment for the diffusion processes. The secreted hormones decay over time (destruction) and diffuse through the barriers. Thus, hormone levels will always be higher in the compartment at the side which is closer to the nearest obstacle, as these sensors are frequently triggering hormone secretion.

In addition to sensor-induced hormone excretions and diffusion, hormone levels can affect motors or other actuators. Finally hormones can potentially affect the production or the degradation of other hormones, a process which is not used by the examples described in this article. All these processes, sensor-induced secretion, actuator-affection and hormone-to-hormone interactions are only triggered in compartments where local hormone-levels or sensor inputs exceed defined thresholds. These thresholds, together with the hormone-specific constants, are stored in a data structure called 'genome', which will be subject to an Artificial Evolutionary process.

### 3 Model 1: A Simple Obstacle-Avoidance Controller

We here describe a very simple AHHS, which allows a robot to avoid obstacles. We assume a robotic hardware like it is depicted in figure 2 and we assume also the compartmentalization that is depicted in this figure: The robot is equipped with two lateral distance sensors and with two motors. Our controller assumes three compartments in the robot, the left compartment holds the left sensor ( $S_l(t)$ ) and the left motor ( $A_l(t)$ ), the right compartment holds the right sensor ( $S_r(t)$ ) and the right motor ( $A_r(t)$ ). We use here just one single hormone ( $H^1$ ) which is excreted at a base rate of ( $H_{base}^1$ ) and which has a fixed decay rate ( $H_{decay}^1$ ). Our AHHS exploits the fact that the diffusion process together with the decay rate leads to a hormone gradient pointing to the compartment that received an above-threshold sensory input ( $S_x > 40$ ), because a hormone value of  $s^1 S_x$  is added there.  $S_x$  represents a reported sensor value on side  $x \in \{l, r\}$  and  $s^1$  defines how many hormone units are secreted per sensor unit. For the sake of simplicity, we assumed that both sensors report the distance to an obstacle in a linear manner ( $0 \leq \text{sensorvalue} \leq 255$ ). The dynamics of the hormone values in all three compartments are modelled as in equations 1 – 3:

$$\frac{\Delta H_1^1}{\Delta t} = +H_{base}^1 - H_1^1(t)H_{decay}^1 + (S_l(t) > 40)s^1 S_l(t) + D_{1,2}^1(t) \quad (1)$$

$$\frac{\Delta H_2^1}{\Delta t} = +H_{base}^1 - H_2^1(t)H_{decay}^1 + D_{2,1}^1(t) + D_{2,3}^1(t) \quad (2)$$

$$\frac{\Delta H_3^1}{\Delta t} = +H_{base}^1 - H_3^1(t)H_{decay}^1 + (S_r(t) > 40)s^1 S_r(t) + D_{3,2}^1(t) \quad (3)$$

The diffusion of the hormone  $H^i$  at time  $t$  is modeled with the function  $D_{x,y}^i(t)$ , as described in the following equation 4, whereby  $d^i$  represents the constant diffusion coefficient of the hormone  $H^i$ :

$$D_{x,y}^i(t) = \frac{H_y^i(t) - H_x^i(t)}{2} d^i \quad (4)$$

The robot's actuators are activated in correspondence to the local hormone level, as described in equations 5 and 6. Please note that the robot drives straight, if both actuator inputs are of identical value and higher actuator inputs lead to a faster robot. The factor  $a^1$  expresses how much one unit of hormone  $H^1$  increases the actuator inputs.

$$A_l(t) = a^1 H_1^1(t) \quad (5)$$

$$A_r(t) = a^1 H_3^1(t) \quad (6)$$

To test the conservation of mass and the influence of model parameters, we constructed a stock-and-flow representation [5] of our model by using the software tool VENSIM™[16] (see figure 3). This allowed us to investigate the emerging hormone levels under defined regimes of sensor input data and to calculate how motor output will in turn be affected by varying hormone levels.

Using the stock-and-flow model, we investigated the hormone levels that emerge in a modelled robot run, when no obstacles disturbed the robot. We investigated the equilibria that arise when one sensor reports a nearby obstacle. To do this, we simulated a sensor input of  $S_l(t) = 70$  from time step  $t = 500$  to time step  $t = 750$ , and a sensor input of  $S_r(t) = 70$  from time step  $t = 1250$  to time step  $t = 1500$ . In all other times, no sensor input was simulated ( $S_l(t) = S_r(t) = 0$ ). These two 'sensor input pulses' were aimed to mimic simple sensor data as it can arise from sensing an obstacle on one side of the robot.

The altered equilibria in times of sensor inputs led to modulated motor inputs, which steer the robot away from the obstacle. After some time the path of the robot is clear again and the controller approaches its initial state (see figure 4a,b). Thus, the motor-sensor loop represents an important external feedback loop, which is part of the homeostatic control loop that regulates the corresponding hormone. The only way for the robot to reach the equilibrium point again is to exert a behaviour that in turn leads to a new sensor input which allows the hormone

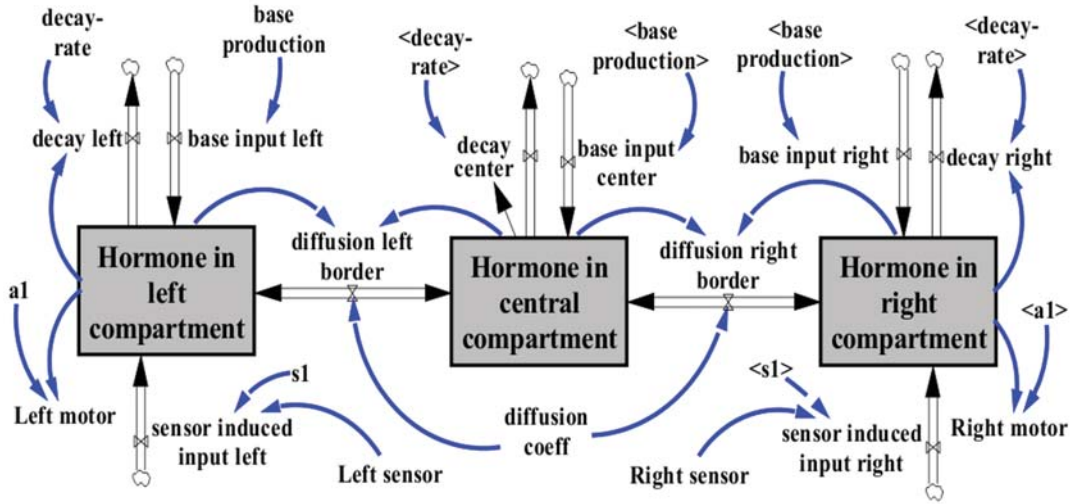


**Figure 3:** Stock-and-flow diagram of our simple AHHS controller. Boxes indicate 'stocks', which can hold (and accumulate) quantities. Double arrows indicate flows, through which quantities can shift from one stock to another. The cloud-like symbols indicate sources and sinks, through which quantities can enter the system or leave the system. Blue arrows indicate causal relationships in the manner or: 'A affects B'.

Parameter/Variable	Value	Units
$H_{base}^1$	20	volume units per step
$H_{decay}^1$	0.1	1 per step
$H_{i \in \{1,2,3\}}^1$	0	volume units
$a^1$	0.05	motor units per volume unit
$s^1$	1	volume units per sensor unit
$d^1$	0.25	dimensionless

**Table 1:** Parameters used in our stock-and-flow model.

level to converge to the homeostatic set point again. Table 1 shows the values we used for our stability analysis and sensitivity analysis of our stock-and-flow model. To test whether or not our AHHS controller will act stable if only noisy sensor data is available, we added a uniformly distributed noise of  $\pm 50\%$  to all sensor data in our stock-and-flow model and depicted the resulting hormone levels and actuator responses. As can be seen in figure 4c,d, even high levels of sensor noise do not lead to significantly disturbed motor output.

After we found that sensor noise cannot disturb the system significantly, we investigated the controller's sensitivity to the major constant parameters, which are: decay rate of the hormone and its diffusion rate. The upper two sub-figures of figure 5 show that the parameter decay rate ( $H_{decay}^1$ ) affects the motor outputs significantly, as a low decay rate leads to a high homeostatic set point for the corresponding hormone  $H^1$ . But what is more important with a robot that moves with a differential drive is the ratio between the two motor outputs, as the more difference there is, the stronger the robot will turn in a curve. We calculated the ratio between the two motor outputs with the two following equations 7 and 8. Using these equations, we performed gain a sensitivity analysis, using the same parameter range as in the analysis mentioned above:

$$R_{left:right} = \frac{A_l(t)}{A_l(t) + A_r(t)} \quad (7)$$

$$R_{right:left} = 1 - R_{left:right} \quad (8)$$

The lower two sub-figures of figure 5 show that this important ratio of motor outputs is not affected at the same order of magnitude than it looks like when one considers each single motor output alone. Thus, the model shows that lowered decay rates of motor-driving hormones will lead mostly to faster driving robots. The controllers ability to turn the robots are not very sensitive to the value of the parameter  $H_{decay}^1$ .

After investigating the controllers sensitivity to the parameter  $H_{decay}^1$ , we performed another sensitivity analysis on the diffusion coefficient of the  $H^1$  hormone, which is  $d^1$ . Figure 6 shows a significantly lower sensitivity of the motor activation (movement speed) but an increased sensitivity of the motor-speed-difference (steering behaviour) to the diffusion coefficient, compared to the sensitivities observed by scaling the decay rates.

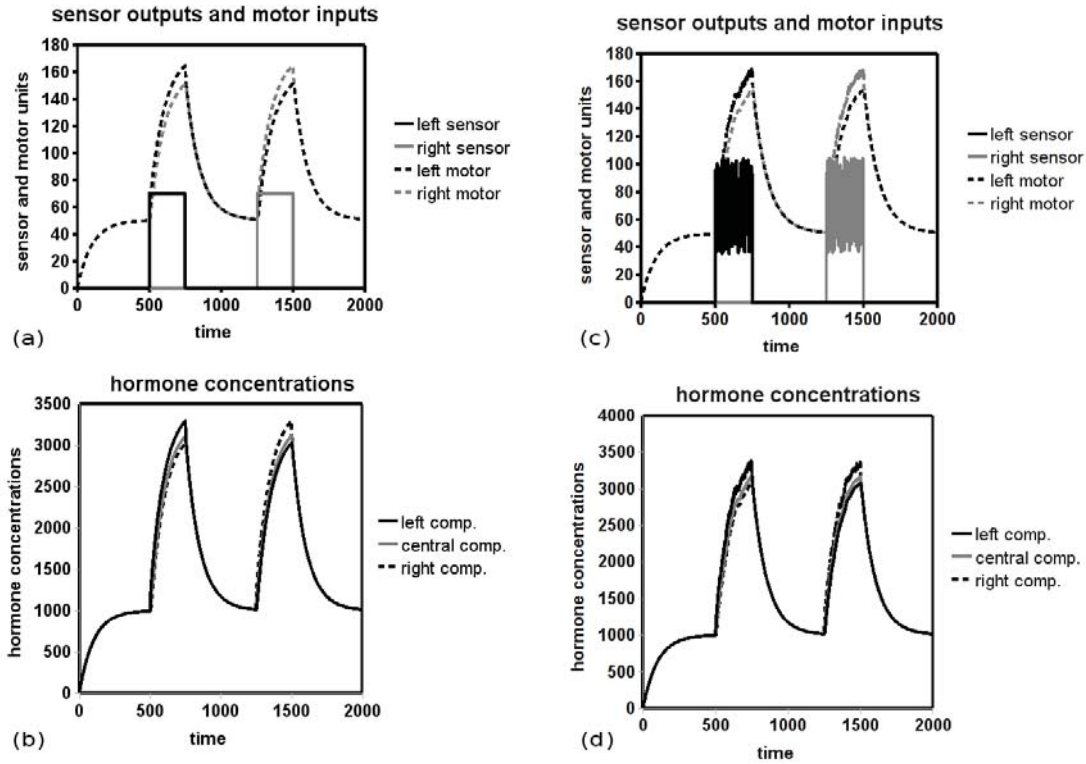


**Figure 4:** (a) Dynamics of sensor values and resulting motor inputs (no sensor noise). (b) Corresponding dynamics of hormone concentrations in the three compartments (no sensor noise). (c) Dynamics of sensor values and resulting motor inputs ( $\pm 50\%$  sensor noise). (d) Corresponding dynamics of hormone concentrations in the three compartments ( $\pm 50\%$  sensor noise).

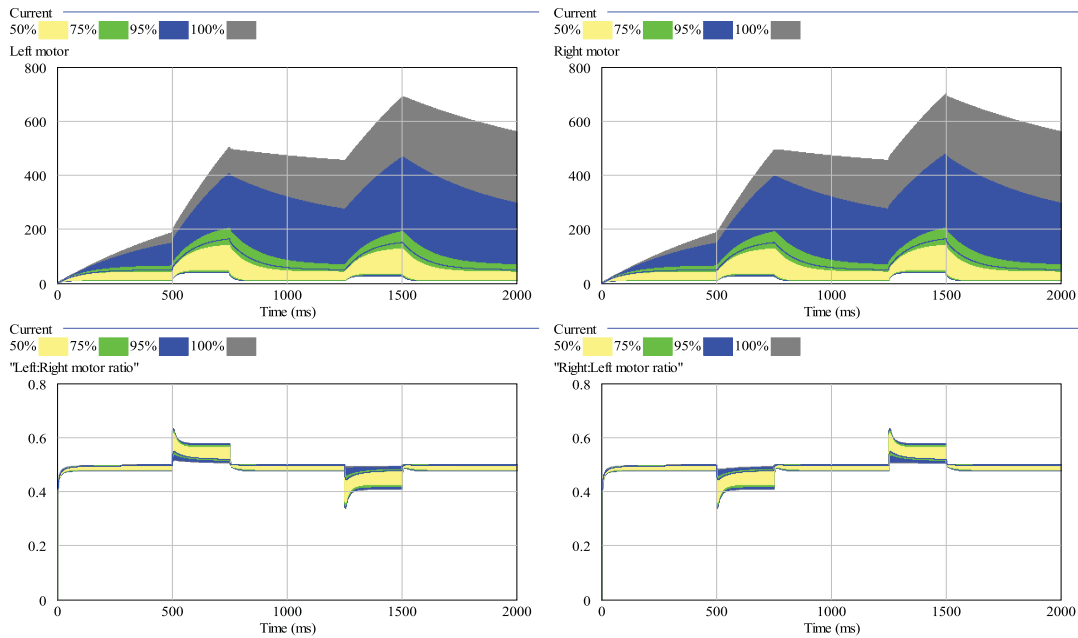


**Figure 5:** Sensitivity analysis of the parameter 'decay rate' ( $H^1_{decay}$ ). 200 independent simulation runs sampled  $H^1_{decay}$  between 0.001 and 0.05: Left upper picture: Resulting left motor outputs. Right upper picture: Resulting right motor outputs. Left lower picture: Resulting ratio between left and right motor output (0.5 means equal output, thus straight driving). Lower right picture: Resulting ratio between right and left motor output. The coloured areas show the range of results that was found in varying the focal parameter. The wider the coloured area is, the higher is the sensitivity of the model to the tested parameter. Quartiles and percentiles are colour-coded, e.g. within the yellow band 50% of all results are located.

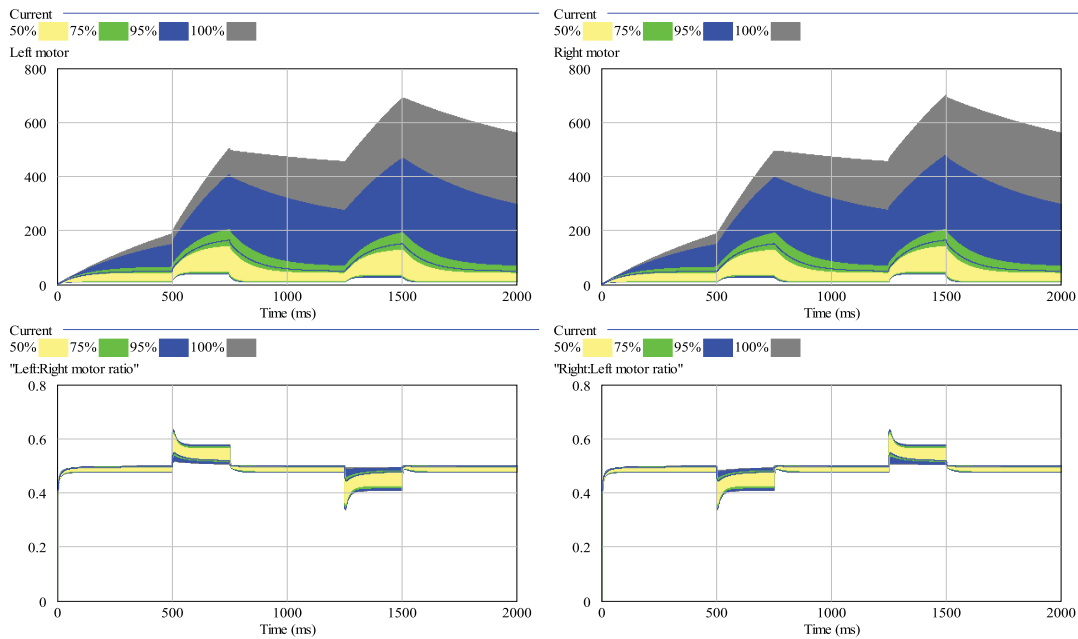


**Figure 6:** Sensitivity analysis of the diffusion coefficient  $d^1$ . 200 independent simulation runs sampled  $d^1$  between 0.01 and 0.5: Left upper picture: Resulting left motor outputs. Right upper picture: Resulting right motor outputs. Left lower picture: Resulting ratio between left and right motor output (0.5 means equal motor output, thus straight driving). Lower right picture: Resulting ratio between right and left motor output.

The analysis of the stock-and-flow model showed interesting findings about the controllers stability and sensitivity. In a test run with a multi-agent simulation of an autonomous robot, we wanted to see the controller act in a structured habitat. The simulator used a model of a robot, as it is depicted in figure 2 and a controller, as it is described in the section above. In the simulations shown here, a noise of  $\pm 20\%$  was applied to all sensor inputs. Figure 7 shows that the robot was able to perform the obstacle avoidance task in an heterogeneous environment, in which various walls and columns blocked the robot's way. Although the controller performed quite well, several collisions with obstacles occurred. Nevertheless, most obstacles were avoided successfully and the robot was always able to free itself after a collision.

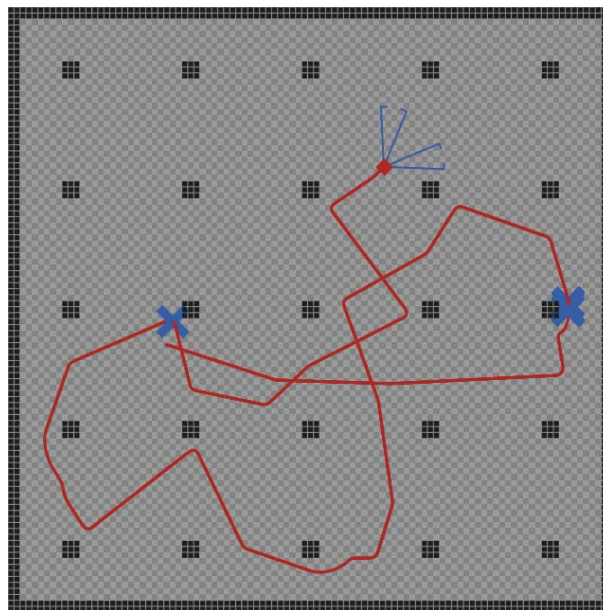


**Figure 7:** The described simple AHHS controller navigated the simulated robot safely through a highly structured environment. Collisions with obstacles occur rarely. Black boxes indicate obstacles and walls. The red rectangular box indicates the robot. The red line shows the robot's trajectory. Blue crosses indicate collisions with obstacles. Two blue cones indicate the area covered by the two sensors. For settings of the controller, see text.

## 4 Model 2: Using two Hormones for a Better Obstacle Avoidance

To better exploit the potential of the differential drive, we extended our AHHS controller in the following way: We introduced now a second hormone, whereby the hormone  $H^1$  is excreted only according to the left sensor input into the left compartment, thus this hormone has now a dedicated meaning: 'There is an obstacle to the left'. The hormone  $H^2$  is excreted only according to the right sensor input into the right compartment, meaning: 'There is an obstacle to the right'.  $H^1$  activates now only the left motor and  $H^2$  activates now only the right motor. In addition to that, the hormones decrease the activation of the contra-lateral side: Those hormone volumes of  $H^1$  that diffused to the right compartment now deactivate the right motor (linear) proportionally and the diffused volumes of  $H^2$  deactivate the left motor. Deactivation can even lead to back-wards driving wheels if the deactivation is bigger then the activation. This way it gets possible that both wheels are driven in opposite directions, what leads to a robot that spins on place without travelling. We assumed that this additional behaviour can decrease the likelihood of obstacle collisions significantly, compared to the first controller, which allowed no change in direction without forward movement. Figure 8 shows a stock-and-flow representation of the enhanced AHHS model, which was then analysed in the software tool Vensim <sup>TM</sup>[16].

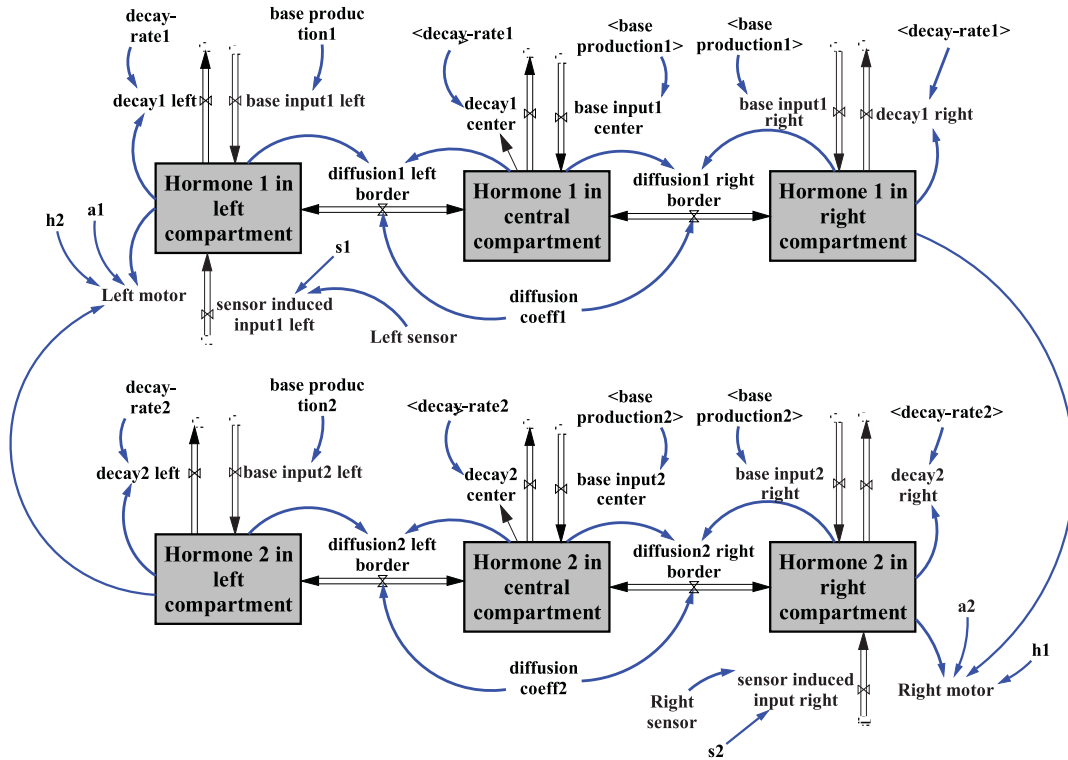


**Figure 8:** Stock-and-flow diagram of our enhanced AHHS controller. The model requires now 6 different stocks, because two hormones have to be modelled in 3 compartments. There is neither a flow from the upper stock to the lower stocks, nor in the other direction. This is because hormones are never converted into other hormones in our AHHS. But, as described in the text, both hormones can modulate actuators in different directions simultaneously, as can be seen by the leftmost and the by the rightmost blue arrow. Boxes indicate 'stocks', which can hold (and accumulate) quantities. Double arrows indicate flows, through which quantities can shift from one stock to another. The cloud-like symbols indicate sources and sinks, through which quantities can enter the system or leave the system. Blue arrows indicate causal relationships in the manner or: 'A affects B'.

The new model is now formulated as follows, see equations 9 – 14, which are mainly based on equations 1 – 3, except that one sensory input was removed for each hormone. The modelling of the diffusion process remained unchanged, according to equation 4.

$$\frac{\Delta H_1^1}{\Delta t} = +H_{base}^1 - H_1^1(t)H_{decay}^1 + (S_l(t) > 40)s^1 S_l(t) + D_{1,2}^1(t) \quad (9)$$

$$\frac{\Delta H_2^1}{\Delta t} = +H_{base}^1 - H_2^1(t)H_{decay}^1 + D_{2,1}^1(t) + D_{2,3}^1(t) \quad (10)$$

$$\frac{\Delta H_3^1}{\Delta t} = +H_{base}^1 - H_3^1(t)H_{decay}^1 + D_{3,2}^1(t) \quad (11)$$

Parameter/Variable	Value	Units
$H_{base}^1$	20	volume units per step
$H_{base}^2$	20	volume units per step
$H_{decay}^1$	0.1	1 per step
$H_{decay}^2$	0.1	1 per step
$H_{i \in \{1,2,3\}}^1$	0	volume units
$H_{i \in \{1,2,3\}}^2$	0	volume units
$a^1 = a^2$	0.05	motor units per volume unit
$s^1 = s^2$	1	volume units per sensor unit
$d^1 = d^2$	0.075	dimensionless
$h^1 = h^2$	0.075	dimensionless

**Table 2:** Parameters used for analysing our enhanced AHHS controller.

$$\frac{\Delta H_1^2}{\Delta t} = +H_{base}^2 - H_1^2(t)H_{decay}^2 + D_{1,2}^2(t) \tag{12}$$

$$\frac{\Delta H_2^2}{\Delta t} = +H_{base}^2 - H_2^2(t)H_{decay}^2 + D_{2,1}^2(t) + D_{2,3}^2(t) \tag{13}$$

$$\frac{\Delta H_3^2}{\Delta t} = +H_{base}^2 - H_3^2(t)H_{decay}^2 + (S_r(t) > 40)s^2 S_r(t) + D_{3,2}^2(t) \tag{14}$$

The activation of motors was changed significantly compared to the first controller model (see equations 5 – 6).

$$A_l(t) = a^1 H_1^1(t) - h^2 H_1^2(t) \tag{15}$$

$$A_r(t) = a^2 H_3^2(t) - h^1 H_3^1(t) \tag{16}$$

We investigated the sensitivity of the enhanced AHHS controller to the two most important parameters: As can be seen in figure 9 and in figure 10, the improved controller showed to be less sensitive to these parameter values.

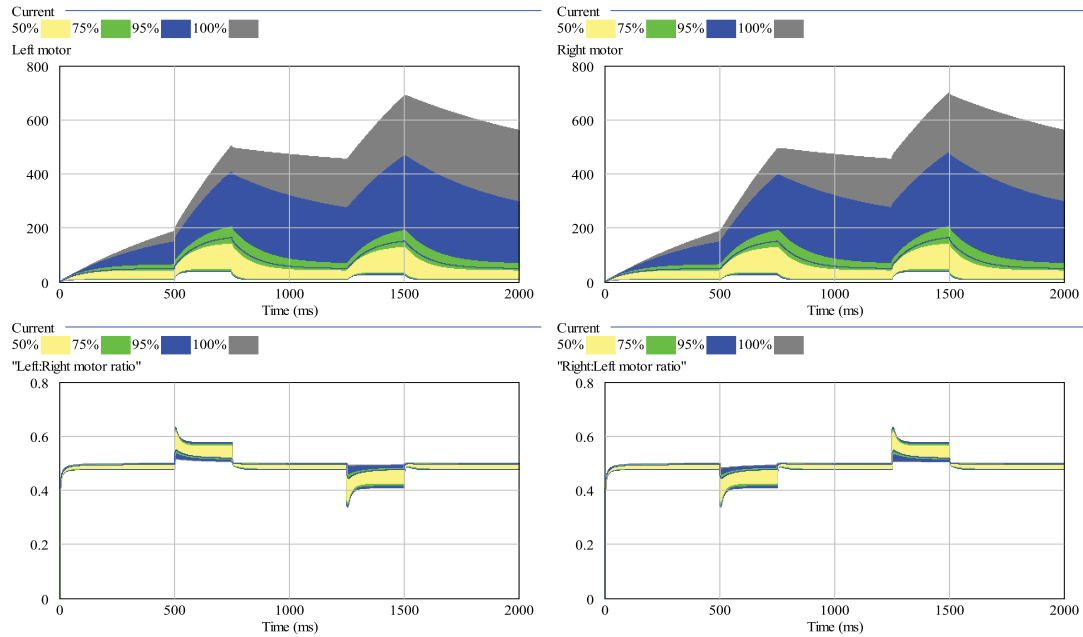


**Figure 9:** Sensitivity analysis of the decay rates  $H_{decay}^1$  and  $H_{decay}^2$ . 200 independent simulation runs sampled both decay rates between 0.001 and 0.05 (both rates were always equal in each run): Left upper picture: Resulting left motor outputs. Right upper picture: Resulting right motor outputs. Left lower picture: Resulting ratio between left and right motor output (0.5 means equal output, thus straight driving). Lower right picture: Resulting ratio between right and left motor output.

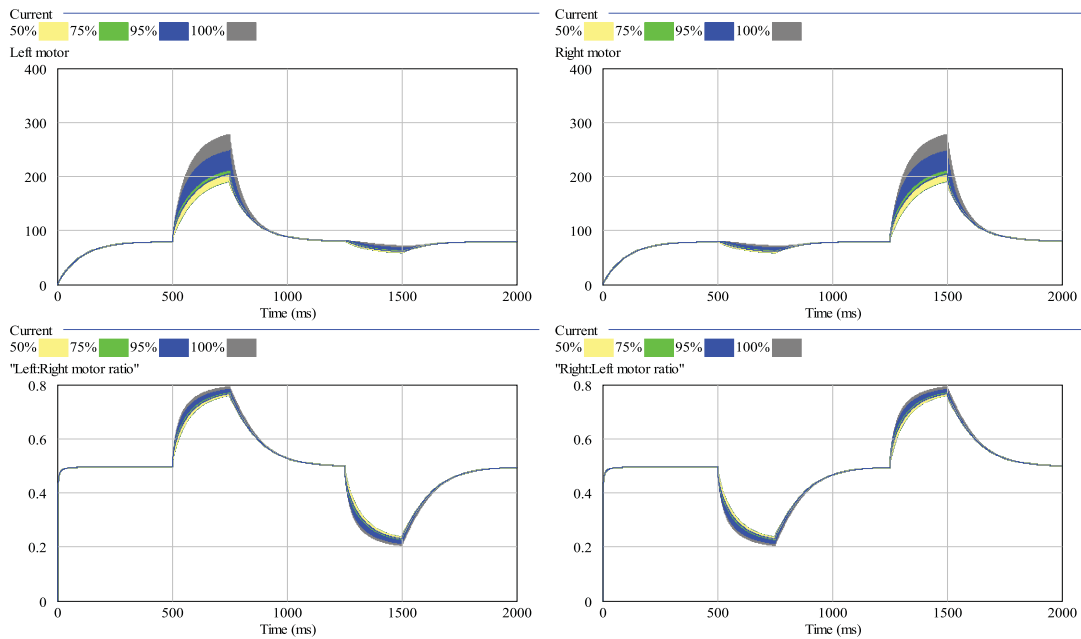


**Figure 10:** Sensitivity analysis of the diffusion coefficients  $d^1$  and  $d^2$ . 200 independent simulation runs sampled  $d^1$  and  $d^2$  between 0.01 and 0.5 (both coefficients were always equal in each run): Left upper picture: Resulting left motor outputs. Right upper picture: Resulting right motor outputs. Left lower picture: Resulting ratio between left and right motor output (0.5 means equal motor output, thus straight driving). Lower right picture: Resulting ratio between right and left motor output.

For a final test run, we implemented the enhanced AHHS controller also in a multi-agent simulation, and observed a simulated robot driving for 10000 time steps through a highly structured habitat: The arena was bound by walls and several columns blocked the robot's way. As expected the robot managed to navigate in this habitat successfully (see figure 11).

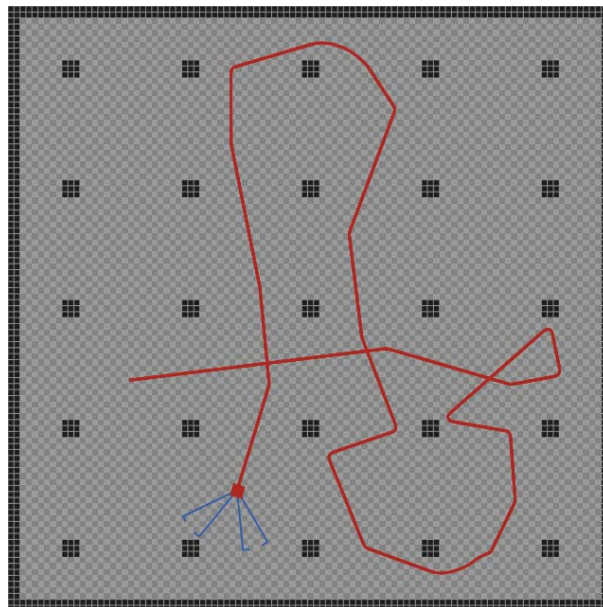


**Figure 11:** The enhanced AHHS controller navigated the simulated robot safely through a highly structured environment without colliding with an obstacle. Black boxes indicate obstacles and walls. The red rectangular box indicates the robot. The red line shows the robot's trajectory. Two blue cones indicate the area covered by the two sensors. For settings of the controller, see text.

## 5 Discussion

We successfully demonstrated how an AHHS controller can navigate autonomous robots in various habitats. We mathematically described our AHHS controllers in a formal way and showed several parameter sets that lead to obstacle avoidance behaviours of varying quality. The examples shown in this article are exemplary 'proof of concepts', obviously many other behaviours can be constructed by different rules in AHHS controllers. Our main focus is 'Evolutionary Robotics' [4] [3], and AHHS controllers provide multiple advantages for such an approach: It is easy to evolve AHHS, because only simple checks have to be performed after mutation and cross-overs to ensure that mutated/mixed AHHS controllers are valid. AHHS controllers provide smooth search landscapes for 'Evolutionary Computation' and novel mutation operators can be tested: e.g., hormones can be easily switched on or off in the 'Artificial Genome'.

Valentino Braitenberg [2] demonstrated that simple, in his case hard-wired' sensory-inputs can effectively navigate a moving machine (robot) to (or away from) a pre-designed target, mainly by exploiting environmental gradients that point towards that target (light, sound, temperature). The idea of homeostatic control of animal-inspired machines was already a major core component of 'cybernetics', as it was described by Norbert Wiener in the 1950's [18]. It assumes communication [13] [8] of sensor values to central 'control components' which exert positive and negative feedback via actuators back to the sensor input. In contrast to Wiener's approach, who focussed mainly on predicting future positions of a mobile target and on autonomously approaching such targets, our implementation is more focussed on keeping the internal status of our focal robots by forcing them to show the desired behaviours. Our AHHS manipulate the behaviour of the robots in a way that they achieve internal homeostasis of intrinsic hormone levels by moving away from obstacles, which disturb homeostatic set-points by triggering additional hormone secretion. Nevertheless, our approach follows the idea of 'cybernetics' and can thus be called a cybernetic regulation achieved by virtual hormones: Also 'cybernetics' involves a sort of filtering of sensory input, as it can be seen by our hormones, which integrate past sensory input over time. Even  $\pm 50\%$  sensor noise did not affect hormone levels significantly. An important feature of our AHHS is the steady decay of such integrated information, as it is modelled by the hormones decay rate. This allows 'forgetting' of outdated information, as long as it is not reinforced by new sensory input.

Another important feature of our controller is the compartmentalization of our robot's virtual inner space. These compartments allow 'computation in space', because sensors and actuators are linked to those compartments that correspond to their position on the robot. This can be seen by the fact that we could use just one single hormone for avoiding obstacles at the left and obstacles at the right. It was the combination of compartmentalization, decay processes and diffusion processes that allowed one single hormone to regulate navigation into both directions.

Several studies suggest also hormone-inspired control for autonomous robots: The studies of [14] suggest a hormone-based system, but in those systems hormones are more like messages that are routed among several robots. In our AHHS, hormones are modeled like chemical substances, which flow through a virtual (robotic) organism. For example, in our approach the 'conservation of mass' is a feature that was important for us. As can be seen by the stock-and-flow diagram in figure 3, the conservation of mass is guaranteed in our AHHS models. Another variant of hormone-inspired control was suggested by [6] [1]. In contrast to those models, our hormone controllers regulate the whole behaviour of the robot alone, in contrast to that the other approaches use the hormones to modulate an underlying Artificial Neural Network. Such a hormonal control scheme was also suggested in another study [17], where a hormone-model was used to express 'moods' of the robot and triggering/affecting different pre-programmed and hand-coded behavioural controllers. Thus, to our knowledge, our AHHS controller is the first robot controller that simulates endocrine processes in the way it is modelled in the previous sections and which regulates the behaviour of the robots without any other controlling structure or pre-programmed functionality.

We suggested a novel concept for engineering a controller for autonomous robots. So far, we investigated a system of difference equations. By using 4th-order Runge-Kutta method, we can also investigate our model like it was a set of differential equations. Additional individual-based simulations allowed us to test the controller in environments with increased complexity. It showed that our controller acts stable, fulfils the given task and can deal with high levels of sensor noise. Our further work will test the AHHS to control joined multi-modular robotic organisms in simulation and on real robotic hardware.

## 6 Acknowledgements

Thomas Schmickl is supported by the following grants: EU-IST FET project 'I-SWARM', no. 507006 and the FWF research grant no. P19478-B16, EU-IST FET project 'SYMBRION', no. 216342, EU-ICT project 'REPLICATOR', no. 216240.

## 7 References

- [1] Orlando Avila-García and Lola Cañamero. Hormonal modulation of perception in motivation-based action selection architectures. In Lola Cañamero, editor, *Agents that Want and Like: Motivational and Emotional Roots of Cognition and Action, Symposium of the AISB '05 Convention, University of Hertfordshire, UK, April 14-15, 2005.*, pages 700–712, 2005.
- [2] Valentino Braitenberg. *Vehicles: experiments in synthetic psychology*. MIT Press, Cambridge, MA, 1984.
- [3] Dario Floreano, Peter Dürri, and Claudio Mattiussi. Neuroevolution\_ from architectures to learning. *Evolutionary Intelligence*, 1:47–62, 2008.
- [4] Dario Floreano, Phil Husbands, and Stefano Nolfi. Evolutionary robotics. In Bruno Siciliano and Khatib Oussama, editors, *Handbook of Robotics*, pages 1423–1452. Springer, Berlin, 2008.
- [5] Jay .W. Forrester. *World Dynamics*. Wright-Allen, Cambridge, Massachusetts, 1971.
- [6] Mark Neal and John Timmis. Timidity: A useful mechanism for robot control? *Informatica*, 4(27):197–204, 2003.
- [7] David Payton, Mike Daily, Regina Estowski, Mike Howard, and Craig Lee. Pheromone robotics. *Autonomous Robots*, 11(3):319–324, November 2001.
- [8] John R. Pierce. *An Introduction to Information Theory. Symbols, Signals and Noise*. Dover Publications, Inc., New York, Cambridge, MA, 1980.
- [9] REPLICATOR. Project website, 2008. <http://www.replicators.eu/>.
- [10] Swarm Robot. Project website, 2007. <http://www.swarmrobot.org/>.
- [11] Thomas Schmickl and Karl Crailsheim. Trophallaxis within a robotic swarm: bio-inspired communication among robots in a swarm. *Autonomous Robots*, 25:171–188, 2008.
- [12] Jörg Seyfried, Marc Szymanski, Natalie Bender, Ramon Estaña, Michael Thiel, and Heinz Wörn. The I-SWARM project: Intelligent small world autonomous robots for micro-manipulation. In Erol Şahin and William M. Spears, editors, *Swarm Robotics Workshop: State-of-the-art Survey*, pages 70–83. Springer-Verlag, 2005.
- [13] Claude E. Shannon. A mathematical theory of communication. *Bell System Technical Journal*, 27:79–423, July and October 1948.
- [14] Wei-Min Shen, Behnam Salemi, and Peter Will. Hormone-inspired adaptive communication and distributed control for CONRO self-reconfigurable robots. In *Transactions on Robotics and Automation*, pages 700–712. IEEE, 2002.
- [15] SYMBRION. Project website, 2008. <http://www.symbion.eu/>.
- [16] Ventana Systems. Vensim™. <http://www.vensim.com>.
- [17] Shigeki Sugano Tetsuya Ogata. Emotional communication robot: Wamoeba-2r emotion model and evaluation experiments. In *Proceedings of the International Conference on Humanoid Robots (Humanoid 2000)*, 2000.
- [18] Norbert Wiener. *Cybernetics: or Control and Communication in the Animal and the Machine*. MIT Press, Cambridge, MA, 1948.